An Operational Ocean Color Approach with *Végétation/SPOT-4*

Bertrand Fougnie*, Patrice Henry* and Philippe Gaspar**

* Centre National d'Etudes Spatiales, *Toulouse, France*.
** Collecte Localisation Satellite, *Ramonville St-Agne, France*.

ABSTRACT

Demand for near-real-time satellite ocean observations is rapidly increasing with the development of operational oceanography and its applications such as ocean monitoring for offshore oil exploitation, fish resources management or detection of surface pollution. Ocean color is one of the few important ocean properties measurable from space. *Végétation*, launched on-board *SPOT-4* in 1998, is a push-broom sensor equipped with 4 wide field-of-view cameras corresponding to 4 spectral bands : blue, red, near-infrared and SWIR bands. Unlike SeaWiFS or MODIS, *Végétatio*n was not designed for ocean color studies. Nevertheless, we demonstrate here that useful ocean color measurements can de deduced from the *Végétation* blue band, the only that is significantly sensitive to the marine reflectance. The main processing steps include : i/ correction for gaseous absorption, ii/ correction for molecular scattering which represents, for the blue band up to 90% of the total observed radiance, and iii/ correction for aerosol scattering. *Végétation* system being fully operational, near-real-time ocean color observations can thus be obtained with this instrument. The first results, concerning a limited ocean region, are presented and compared with SeaWiFS and radar altimeter observations.

1. INTRODUCTION

Demand for near-real-time (NRT) satellite ocean observations is rapidly increasing with the development of operational ocean monitoring and forecasting systems. NRT oceanic information is crucially needed to provide efficient vessel routing based on actual currents, to monitor powerful eddies that can damage offshore oil-production platforms, to detect surface pollution and allow quick reaction, or to locate plankton-rich waters that can offer favorable fishing grounds. Ocean color is one of the few ocean properties measurable from space and thus an important contributor to global ocean monitoring systems. Several ocean color sensors were launched in the last five years : MOS, SeaWiFS, OCI, OCM, MODIS. But the data from most of them are not readily available for near-real-time applications or only cover limited geographic areas. Unlike these instruments, *Végétation* was not designed for ocean color measurements. *Végétation*, however, offers global data acquisition and a fully operational ground segment delivering timely products. We demonstrate in this paper that ocean color measurements can be deduced from the *Végétation* blue band. These measurements can usefully complement other ocean observations for various operational purposes.

2. DESCRIPTION OF THE VEGETATION SYSTEM

2.1 Instrumental description

The *Végétation* instrument was launched in April 1998 on-board the SPOT-4 satellite. It is composed of 4 cameras, each of them composed of a wide field-of-view optic with telecentric lens, a spectral band and an acquisition line of 1728 detectors. The total field-of-view is 101° cross track leading to a ground swath of 2250 km and the ground resolution of about 1km at nadir is almost constant over the entire field-of-view. The four complementary spectral bands are the blue band (B0 from 0.43 to 0.57 μm), the red band (B2 from 0.61 to 0.68 μm), the near-infrared band (B3 from 0.79 to 0.89 μm), and the short-wave infrared band (SWIR from 1.58 to 1.75 μm). The spectral bands B2, B3, and SWIR, identical to the HRVIR/SPOT-4 spectral bands, were designed for the vegetation monitoring, B2 centered on the absorption peak of the chlorophyll, B3 corresponding to the maximum vegetation spectral reflectance, and SWIR which is very sensitive to water content. An additional blue band was defined for atmospheric correction. *Végétation* is equipped with an on-board calibration device useful for various aspect such as multi-temporal and multi-angular calibration or radiometric noise estimation.

Moreover, *Végétation* is designed to be independent of its host satellite and, in addition of the imaging instrument, it includes its own recording, transmission and management equipments. A detailed description is given in *Pulitini et al* (1994).

2.2 Instrumental performances

The absolute calibration of *Végétation* is described in *Meygret et al*. (2000) and *Henry and Meygret* (2000). It is performed with different and complementary methods based on ground measurements, on-board calibration system, vicarious calibration over test sites, calibration over natural targets (ocean or desert sites, sun glint, clouds) and finally cross-calibration with other sensors (HRVIR, POLDER). The multi-angular calibration aspect important for wide field-of-view sensors is described in *Fougnie et al.* (2000). Finally, the estimated accuracy is estimated at about 5% in absolute calibration and 2-3% in inter-band calibration. The geometric performances mainly composed by the absolute location accuracy, the multi-spectral registration, and the multi-temporal registration are fully described in *Sylvander et al*. (2000). The absolute location is estimated better than 500 m, and the multi-spectral registration at about 0.2 pixel. The noise equivalent reflectance estimated for *Végétation* and for the very small radiances are less than 0.2 $W/m^2/sr^1/\mu m^1$ in all the spectral bands (which is comparable for instance to OCTS and CZCS, *IOCCG*, 1998). As if *Végétation* is not designed for ocean color studies, it appears that the available spectral bands, the calibration accuracy and radiometric performances are quite consistent with ocean color requirements for open ocean as written by *IOCCG* (1998) and not only for the radiometric aspects. Only one spectral band is sensitive to ocean reflectance but in theory, it is sufficient to retrieve some information from the surface pigment concentration as described by *Morel* (1988) revised in *Morel and Maritorena* (2001). Ocean color missions such as SeaWiFS, MODIS, POLDER use much more spectral bands, usually between 412 and 565 nm, combining these spectral reflectances in order to reduce some residual atmospheric effect and to improve the sensitivity and accuracy of the bio-optical algorithm. The objective with *Végétation* is not presently to retrieve accurate surface pigment concentration but mainly to draw ocean color maps from regions of interest.

2.3 *Végétation* products

Végétation is not just a payload on-board the SPOT4 satellite, it is a complete system with a specific ground segment for data programming, processing and distribution as described in *Henry* (1999). It allows the availability of images acquired all over the world through its capability of on-board recording and the centralization of the images reception and archiving. Data are produced by the Centre de Traitement des Images *Végétation* (CTIV), located in Mol (Belgium), which is a fully dedicated center in charge of the processing and distribution of *Végétation* products. The delay for image products delivery is very short, typically 2 to 4 days after acquisition date : the service is operational. The data used in our study are composed by VGT-P products in HDF format with ancillary data like geometry of acquisition (viewing zenith and azimuth angles, solar zenith and azimuth angles), and exogenous atmosphere information like vertically integrated ozone and water vapor content. The VGT-P products are related to one image acquisition. In this products, the system errors such as detectors calibration or spectral bands misregistration, are corrected. The physical values are composed by top of the atmosphere reflectances in the four *Végétation* spectral bands. The basis geographic projection for data is a Plate Carrée projection leading to a sampling interval of 1 km at the equator.

3. ATMOSPHERIC CORRECTION ALGORITHM

3.1 Cloud mask

Before trying to define an algorithm to correct the top of the atmosphere (TOA) reflectances of the atmospheric contribution, the first module to develop is an efficient and optimum cloud mask. The SWIR band of *Végétation* is an important advantage for a cloud mask because this spectral band is centered at 1.65 μm where reflectance is related to water content of the observed scene. In addition, ocean and molecules are optically black for this wavelength and consequently the observed signal is only due to clouds, aerosol or sun glint which are the components we want to detect and furthermore eliminate or correct. Finally, it was possible to define an efficient cloud mask simply by applying a threshold on the reflectance observed in the SWIR band : pixel with corresponding TOA reflectance greater than 0.0125 in SWIR band were declared cloudy. In a near future, a more optimized filter would be developed by combining the SWIR information with for example ratios of reflectances from other bands.

3.2 Rayleigh scattering correction

The objective is to transform TOA reflectances of the level-1 products into surface reflectances usually called level-2 products. For this, the TOA reflectance, ρ_{toa}, observed for the spectral band k can be approximated by

$$\rho_{toa} = \left\{ \rho_r + \rho_a + \rho_w \frac{T_s^{tot} \cdot T_v^{tot}}{(1 - \rho_w . \omega)} \right\} . t_g \quad (1)$$

where ρ_r is the reflectance due to molecular scattering, ρ_a is the reflectance due to aerosol scattering including coupling terms with molecules, ω is the atmospheric albedo, T_s^{tot} and T_v^{tot} are total atmospheric transmittances (sum of direct and diffuse components) respectively for the solar and viewing zenith angles, t_g is the transmission due to gaseous absorption (ozone plus water vapor) and ρ_w is the water reflectance. We ignore here the surface foam reflectance which is negligible for surface wind speed under 5-7 $m.s^{-1}$ but this term should be considered is a more general algorithm simply using the surface wind speed from meteorological data set. The molecular contribution can be accurately computed using a radiative transfert code (thereafter called SOS code) based on the Successive Order of Scattering method developed by *Deuzé et al.* (1989). For this, the main input parameter is the equivalent molecular optical thickness, τ_{eq}, calculated for a given *Végétation* spectral band by

$$\tau_{eq} = \frac{P}{P_o} . \frac{\int_\lambda E_s(\lambda).\tau_r(\lambda).t(\lambda).d\lambda}{\int_\lambda E_s(\lambda).t(\lambda).d\lambda} \quad (2)$$

where for the wavelength λ, $\tau_r(\lambda)$ is the molecular optical thickness according *Hansen and Travis* (1974) and *Gordon et al.* (1988), $t(\lambda)$ is the monochromatic instrumental response, $E_S(\lambda)$ is the extraterrestrial solar irradiance, P the surface pressure (P_O = 1013Hpa). For the standard pressure condition P_O, the equivalent molecular optical thickness are presented for each spectral band in Table (1).The gaseous transmittance, t_g, can be calculated using the 6S radiative tranfert code (*Vermote et al*., 1997) using ancillary meteorological data.

Spectral Band	B0	B2	B3-NIR	SWIR
Central wavelength	458 nm	670 nm	820 nm	1640 nm
τ_{eq}	0.20599	0.04691	0.01854	0.001168

Table 1. Equivalent molecular optical thickness and central wavelength for the 4 spectral bands of *Végétation.*

3.3 Aerosol amount determination

It is important to mention that for the blue band, the water contribution that we want to retrieve, ρ_w, represents only about 10 to 20% of the total TOA reflectance, ρ_{toa}, and is for instance nearly equal to the aerosol contribution in standard conditions of the open ocean. Furthermore, after correction of the Rayleigh scattering contribution, the main difficulty is to estimate properly the aerosol contribution. The first approach used in this study is a one-band aerosol determination. Using the near-infrared band B3, for which the ocean reflectance is nearly close to zero and can be neglected (ρ_w(B3)~0 in open ocean), the reflectance, ρ_{toa}(B3) is used to make an estimation of the aerosol amount as described in Eq. (3).

$$\rho_a(B3) \cong \rho_{toa}(B3) / t_g(B3) - \rho_r(B3) \quad (3)$$

For the reason explained here above, it was decided to smooth the TOA reflectance ρ_{toa}(B3) before the estimation of ρ_a(B3) in order to minimize the impact of the instrumental radiometric noise of the B3 band and to avoid the propagation of this radiometric noise on the estimated marine reflectance through the aerosol contribution. Consequently, the TOA reflectance ρ_{toa}(B3) was binned 7 by 7 which attenuate the radiometric noise by a factor of 7, sufficient enough for this application (see results section). Eq. (4), the aerosol reflectance is calculated for B0 by extrapolating the aerosol reflectance estimated at B3 assuming a Maritime 98% aerosol model (thereafter called M98) defined by *Shettle and Fenn* (1979) and

proposed by *Gordon and Wang* (1994) for the SeaWiFS data processing. This extrapolation ε^{M98}(B0,B3), including coupling terms with the molecular contribution, is taken from a look-up table generated using the SOS code referenced above.

$$\rho_a(B0) = \rho_a(B3).\varepsilon^{M98}(B0,B3) \quad (4)$$

Finally, the aerosol contribution can be subtracted to the TOA reflectance measured in the blue band and the water reflectance can be written :

$$\rho_w(B0) = \frac{\rho_s(B0)}{T_s^{tot}(B0).T_v^{tot}(B0) - \omega.\rho_s(B0)} \quad (5)$$

where

$$\rho_s(B0) = \frac{\rho_{toa}(B0)}{t_g(B0)} - \rho_r(B0) - \rho_a(B0) \quad (6)$$

Presently, this first version of the aerosol correction is a one-band determination and estimates the aerosol amount considering only one unique aerosol spectral model. It is obvious that this part of the processing can be improved. For example, it should be possible to use the B2 spectral band, centered at 650 nm, to perform a two-band aerosol determination and try to estimate the aerosol spectral model in addition to the aerosol amount. Nevertheless, in the case of this study, the aerosol M98 provides good preliminary results. For example, it was possible to verify the consistency of our aerosol correction by controlling that the water reflectances restituted for the B2 band (red band) is null.

3.4 Bidirectional effects

Végétation is a wide field-of-view sensor and consequently, because acquisitions are made for various viewing conditions over all its 2200 km swath, some effects due to bi-directionality of marine reflectance may perturb the interpretation of results. The bi-directional effect is small, typically 10 to 20% of the marine reflectance as shown by *Morel and Gentili* (1993), but normalize these marine reflectances to a standard condition should be helpful to avoid difficulties when comparing or merging acquisitions made for 3 or more successive days for which viewing conditions are not necessarily identical. According to *Morel and Gentili* (1996), the marine reflectance estimated for the satellite viewing geometry in Eq. (5), is corrected as following

$$\rho_w(B0) = \frac{\Re_o.f_o.Q(\theta_s,\theta_v,\varphi)}{\Re(\theta_v).f(\theta_s)}\rho_w(B0,\theta_s,\theta_v,\varphi) \quad (7)$$

where ρ_w(B0) is the marine reflectance corrected by directional effects, $\Re$ is a factor including reflection and refraction effects on the air-sea interface for the zenith viewing angle, denoted $\Re_o$ when the zenith angle is zero, Q is the bidirectional function for solar and viewing geometry (*Morel and Gentili*, 1996), and f is the proportional factor between the inherent optical properties and the diffuse marine reflectance (see *Morel*, 1988), f is denoted f_O for null solar zenith angle. We used for the B0 spectral band a Q table initially computed for 443 nm.

4. FIRST RESULTS

4.1 Region of interest

Our site of interest is the Mozambique Channel, between Madagascar and Mozambique. This geographic zone is about 1 million km² and is defined by 35°E to 45°E in longitude and 15°S to 25°S in latitude. The oceanic circulation is important in this region where important fisheries activities occurred and it should be interesting to try to detect the water movements and to try to identify some correlation with altimetry and ocean temperature products. The acquisition dates considered for this study were from June 15th to 17th, 2000 and from July 11th to 20th, 2000 which are globally clear days for this region and for which the sun glint was avoided.

4.2 *Végétation* ocean color product

Images (1) to (4) illustrate the main steps of the atmospheric correction processing for the above region of interest and for the 17th June, 2000. First, the TOA reflectance for the blue band B0 is presented in Image (1). Madagascar (on the right) and Mozambique (on the left) coasts can be identified with in between the Mozambique Channel. In addition to bright clouds on the upper left corner, a milky mask can be discerned on the left-hand part of the image and it corresponds to the atmospheric contribution due to molecular scattering. The signal coming from the ocean surface is very small, typically 10% of the TOA signal. In Image (2) is presented the TOA reflectance for the NIR band B3. The coasts are much more contrasted, the ocean appears black (no marine contribution in the B3 band, except marginally very close to the coast) and the atmospheric molecular scattering is very small (no milky mask contrarily to B0 on Image (1)). The aerosol signal extracted from the B3 band after application of a cloud mask based on the SWIR band is presented in Image (3). The aerosol signal is binned 7 by 7 in order to strongly reduce the radiometric noise. Residual clouds and sub-pixel clouds are assimilated here to Maritime aerosol. Finally, in Image (4) is presented the retrieved marine reflectance after subtraction of atmospheric constituents (molecular scattering + aerosol contribution thanks to B3, Image (3)). The coasts are white, clouds are black and the image is 1km resolution. The aerosol correction seems quite good because no residual effects appear in the vicinity of clouds detected by the cloud mask. Several marine structure are evidenced in all the Mozambique Channel. Image (5) is a zoom on the marine structures around the Bassas da India and Europa Islands : a big whirlpool (with a diameter of typically 300km) on the left, a mushroom at the center, an upwelling on the right, and several various structures which can be interpreted like active circulation of water masses. The parallel oblique lines are artifact due to some residual effects of the radiometric (multi-angular or inter-detector) correction. The vicinity of these two islands is presented Image (6) for another day, one month later the 16th July, 2000, and a lot of marine structures are visible and strongly different than those of Image (5). The high temporal variability is evidenced here and is confirmed by the time series presented Image (7) where, for only 3 days, the upwelling along the Madagascar coast is clearly evolving.

4.2 Comparison to altimetry and SeaWiFS data

Images (9), the marine reflectance derived for the 15th June, 2000 is confronted to surface pigment concentration derived from the SeaWiFS acquisitions of the 16th June, 2000 and distributed by Orbimage (4km resolution), and the weekly mean sea level derived from altimetry measurements by Topex/Poseidon (*Fu et al*., 1994). The structures observed on the *Végétation* image appear on the SeaWiFS image. As shown in Figure (1), marine reflectances are directly correlated with surface pigment concentration and consequently, this explain why low marine reflectance derived on Image 8a) coincide with high pigment concentration on Image 8b) and conversely. In addition, it can be seen that low marine reflectance on Image 8a) are quite well correlated with large deviation from the mean sea surface level on image 8c) (the dark grey corresponds to positive or negative deviation from the mean sea level, up to 20cm). The same conclusions can be deducted from Images (9) where a 4 days time series of marine reflectances derived from *Végétation* are confronted to surface pigment concentration and weekly mean sea level for the mid July, 2000. Finally, the comparison between marine reflectances derived from Végétation acquisitions and pigment concentrations derived from SeaWiFS acquisitions give us good confidence into the quality of the processing.

5. FURTHER IMPROVEMENTS

It was mentioned during the description of this first algorithm that some improvement can be made on the atmospheric correction. It is difficult to implement a cloud mask that can be used universally everywhere on the Earth and on the year. The cloud mask used here was optimized to perform good results on the Mozambique Channel on June and July. It is probably/perhaps not adapted for other ocean and other observation dates. The *Végétation* instrument has 3 spectral bands in red, NIR and SWIR bands that are not sensitive to marine reflectance and that can be used to develop a more elaborated mask, in particular by using spectral ratios. The second major improvement is the aerosol correction. It has been described that only the M98 aerosol model is used. It is obvious that, if this model is representative to the open ocean, it will not be adapted for all oceanic sites. Once again, 3 spectral bands are available to try to make an estimation of the aerosol spectral variation in addition to the aerosol amount.

6. CONCLUSION

The purpose of this study was try to extract marine information (in particular marine reflectance) from the *Végétation* acquisitions. The SWIR spectral band was used to define an efficient cloud mask. The NIR spectral band was used to estimate the amount of aerosol assimilated to Maritime aerosol model. Finally, accurate atmospheric correction was perform on the blue band, the only one that is sensitive to the marine reflectance. Original and rich information were extracted from the blue band. These results were compared to other sources of measurements like surface pigment concentration and sea level. We conclude that accurate marine reflectance can be retrieved from *Végétation* acquisitions over ocean and in the near future, the advantages offered by the fully operational *Végétation* system can be turn to good account to define a product intended for fisheries activities.

REFERENCES

Deuzé, J.-L., M. Herman, and R. Santer, Fourier series expansion of the transfer equation in the atmosphere-ocean system, *J. Quant. Spectrosc. Radiat. Transfer*, vol. 41, pp. 483-494, 1989.

Fougnie, B., P. Henry, F. Cabot, A. Meygret, and M. C. Laubies, *Végétation* Multi-angular Calibration, Earth Observing System V, *Proceedings of SPIE, 2-4 August, San Diego, USA*, Vol. 4135, pp. 331-338, 2000.

Fu, L.-L., E. Christensen, C. A. Yamarone Jr., M. Lefebvre, Y. Menard, M. Dorrer, and P. Escudier, TOPEX/POSEIDON mission overview, *J. Geophys. Res*., vol. 99, pp. 24,369-24,381, 1994.

Gordon, H. R., J. W. Brown, and R. H. Evans, Exact Rayleigh scattering calculations for use with the Nimbus-7 Coastal Zone Color Scanner, *Appl. Opt.*, vol. 27, pp. 862-871, 1988.

Hansen, J. E., and L. D. Travis, Light scattering in Planetary Atmospheres, *Space Sci. Rev*., 16, 527, 1974.

Henry, P, The *Végétation* System : a Global Monitoring System On-Board SPOT4*, Proceedings of the Euro-Asia Space Week on Cooperation in Space*, ESA SP-430, pp 233-239, 1999.

Henry, P., and A. Meygret, Calibration of *Végétation* Cameras on-board SPOT4, *Proceedings of Végétation-2000, 3-6 April, Lake Maggiore, Italy*, pp. 23-31, 2000.

Hagolle, O., P. Goloub, P.-Y. Deschamps, H. Cosnefroy, X. Briottet, T. Bailleul, J-M. Nicolas, F. Parol, B. Lafrance, and M. Herman, Results of POLDER in-flight calibration *IEEE Trans. Geosci. and Remote Sensing*, May 1999, Volume 37, N°3,pp 1550-1566, 1999.

Hooker, S. B., W. E; Esaias, G. C. Feldman, W. W. Gregg, and C. R. McClain, SeaWiFS Technical Report Series: vol. 1, in *An Overview of SeaWiFS and Ocean Color, NASA, Tech. Memo., 104566*, Greenbelt, Md., 1992.

IOCCG, Minimum Requirements for an Operationnal Ocean-Color Sensor for the Open Ocean, Morel, A. (ed.), *Reports of the International Ocean Color Coordinating Group*, No. 1, IOCCG, Dartmouth, Canada, 1998.

Meygret, A., X. Briottet, P. Henry, O. Hagolle, and O. Hagolle, Calibration of SPOT4-HRVIR and *Végétation* cameras over the Rayleigh Scattering, *Proceedings of SPIE, 2-4 August, San Diego, USA*, Vol. 4135, pp 302-313, 2000.

Morel, A., Optical modeling of the upper ocean in relation to its biogenous matter content (Case 1 waters), *J. Geophys. Res*., vol. 93, pp. 10,749-10,768, 1988.

Morel, A., and B. Gentili, Diffuse reflectance of oceanic waters (2): Bi-directional aspects., *Appl. Opt.,* vol. 32, pp. 6864-6879, 1993.

Morel, A., and B. Gentili, Diffuse reflectance of oceanic waters (3): Implication of bidirectionality for the remote-sensing problem, *Appl. Opt.,* vol. 35, pp. 4850-4862, 1996.

Morel, A., and S. Maritorena, Bi-optical properties of oceanic waters, a reappraisal, *J. Geophys. Res.,* Vol. 106 , No. C4 , p. 7163, 2001.

Pulitini, P., M. Barillot, T. Gentet, and JF Reulet, The *Végétation* payload*, Proceedings of International Symposium on Space Optics*, *Garmish*, 1994.

Shettle, E. P., and R. W. Fenn, Models for aerosols of the Lower Atmosphere and Effects of Humidity Variations on Their Optical Properties, *Rep. AFGL-TR-79-0214,* U.S. Air Force Geophysics Laboratory, Hanscom Air Force Base, Mass., 1979.

Sylvander, S., P. Henry, C. Bastien-Thiry, F. Meunier, and D. Fuster, *Végétation* Geometrical Image Quality, *Proceedings of Végétation-2000, 3-6 April, Lake Maggiore, Italy*, pp. 33-44, 2000.

Vermote., E., D. Tanré, J. L. Deuzé, M. Herman, and J. J. Morcrett, Second Simulation of the Satellite Signal in the Solar Spectrum (6S): An Overview, *IEEE Trans. Geosci. and Remote Sensing*, Volume 35, N°3, 1997.

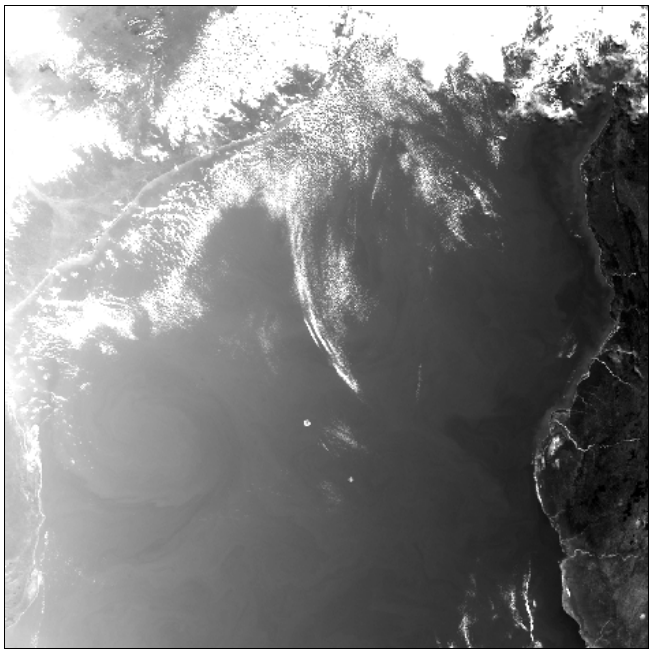

Image 1. TOA refletance for B0 (blue) for the 17th June 2000. One can see Madagascar on the right, Mozambique on the upper left corner. Clouds appear very bright while the molecular scattering produce a 'milky' mask on the image.

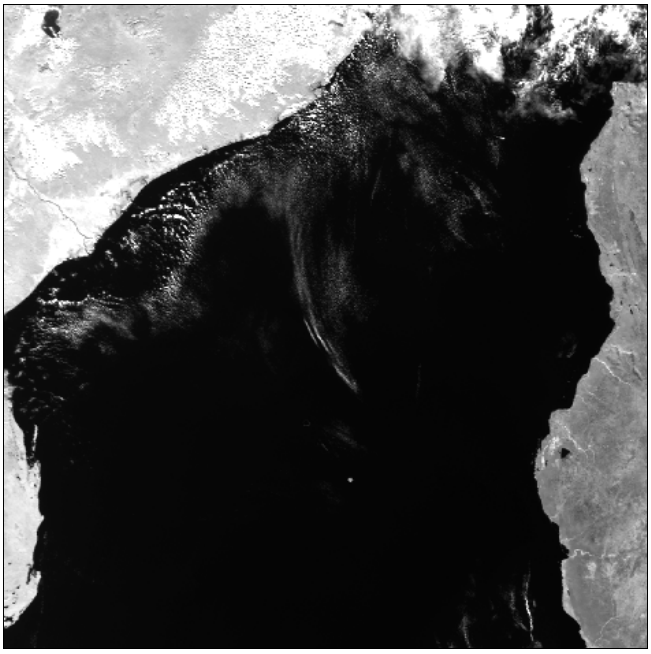

Image 2. Same as image 1 but for the B3 band. Ocean reflectance is null and molecular scattering is small leading to a more contrasted scene between ocean and cosats.

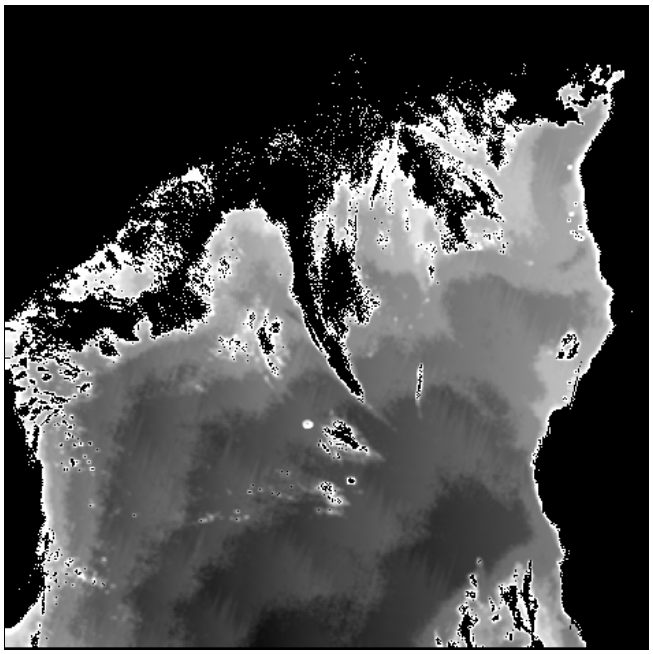

Image 3. Residual signal for B3 after correction of the molecular scattering. This can be assimilated to aerosol or residual clouds signal. The land and clouds are black.

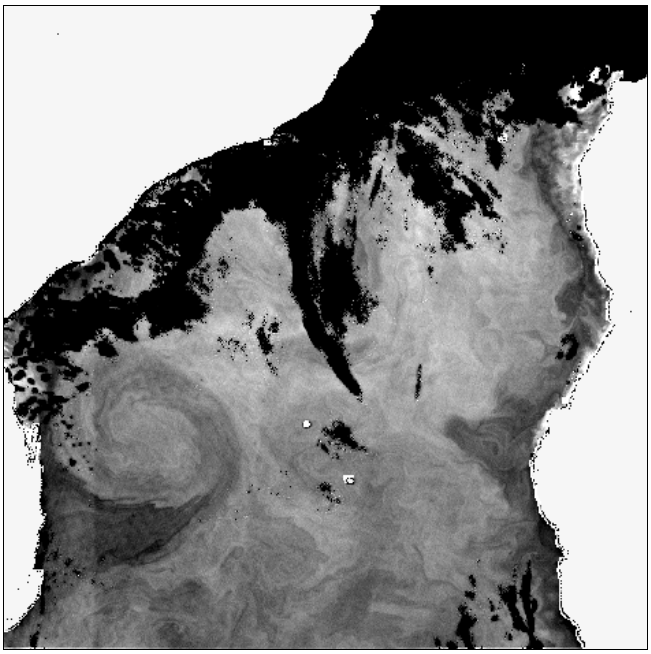

Image 4. Final marine reflectance for B0 after complete atmospheric correction. Land is white and clouds are black. Several marine structures are evidenced. A large whirlpool appears on the left. This whirlpool cannot be easily discerned before processing on Image 1.

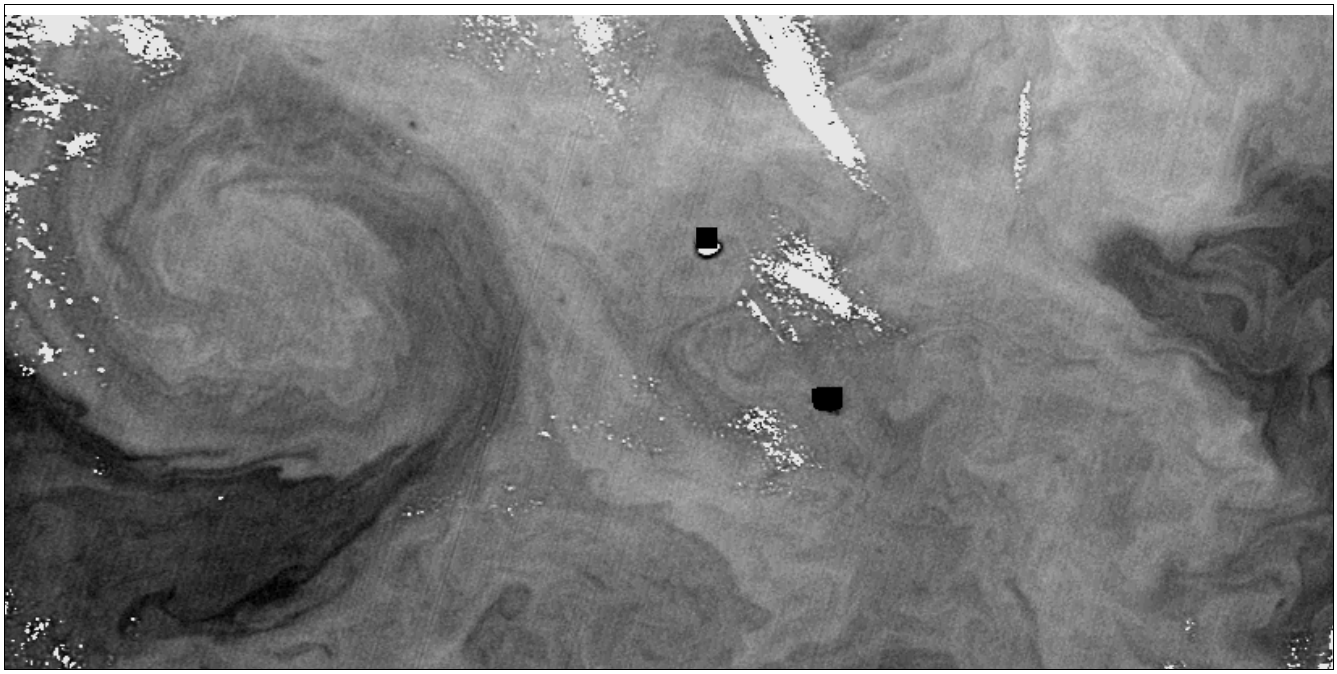

Image 5. Zoom on the marine structures around Bassas da India Island (upper black square at the center) and Europa Island (downer black square at the center) for the 17th June, 2000. Clouds are white on this image.

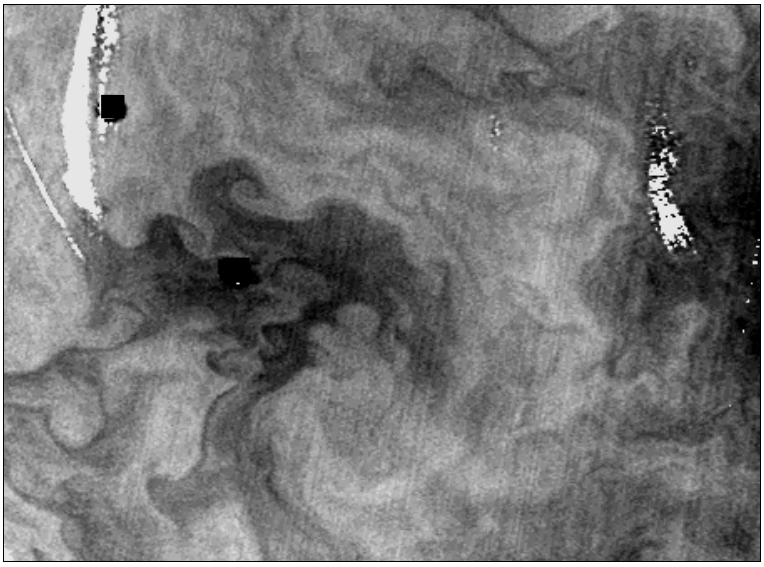

Image 6. Marine structures around the Islands (black squares) mentioned on Image (5) for 16th July, 2000. Clouds are white.

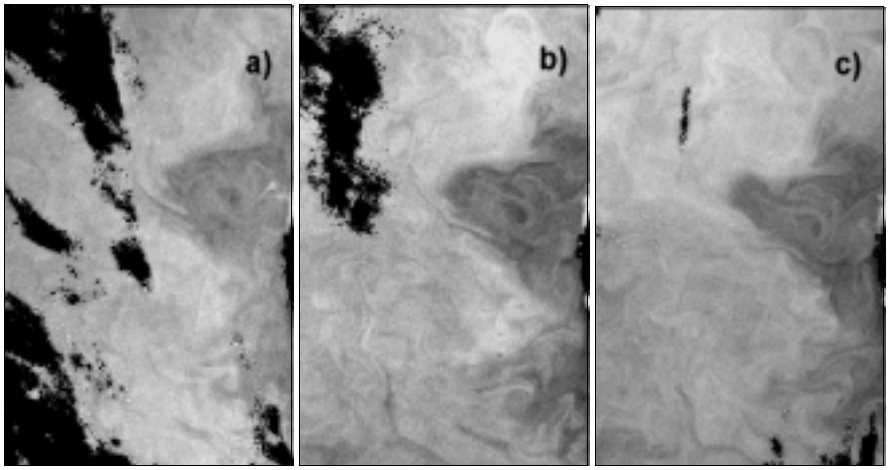

Images 7. Evolution of a structure for 3 days, the 15th June (a), the 16th June (b), and the 17th June 2000 (c), along the Madagascar coast (on the right).

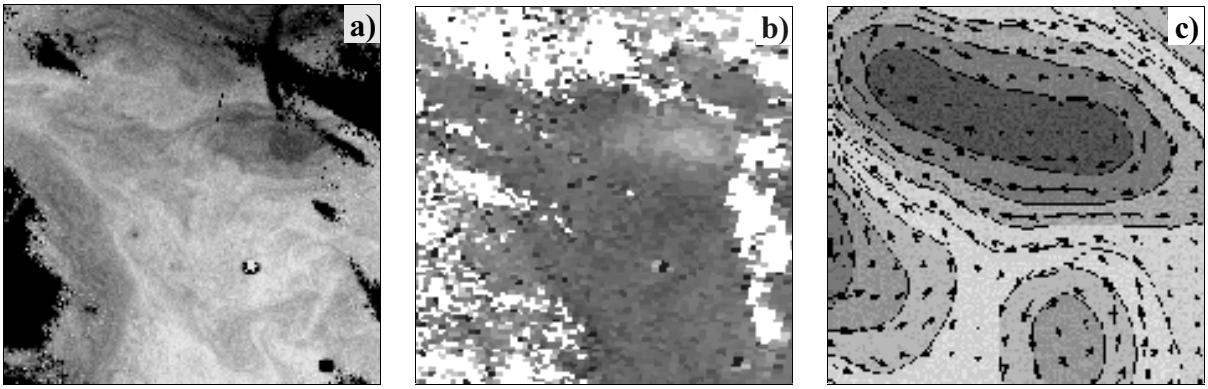

Image 8. The low marine reflectance, derived from the *Végétation* acquisition of the 15th June (a), are consistent with the high pigment concentration derived from SeaWiFS acquisitions for the 16th June (b). In addition, these high marine reflectances, usually called "mushrooms", are correlated to very high or low anomaly of the sea level (in dark grey), typically ± 20 centimeters, as can be seen on the weekly mean altimetry image (c).

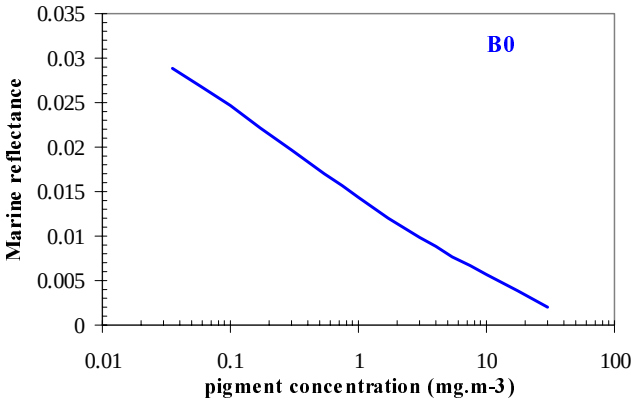

Figure 1. Typical variation of the above-water marine reflectance with the surface pigment concentration in mg.m-3 for the *Végétation* spectral band B0 (equivalent wavelength of 457 nm) according *Morel* (1988)

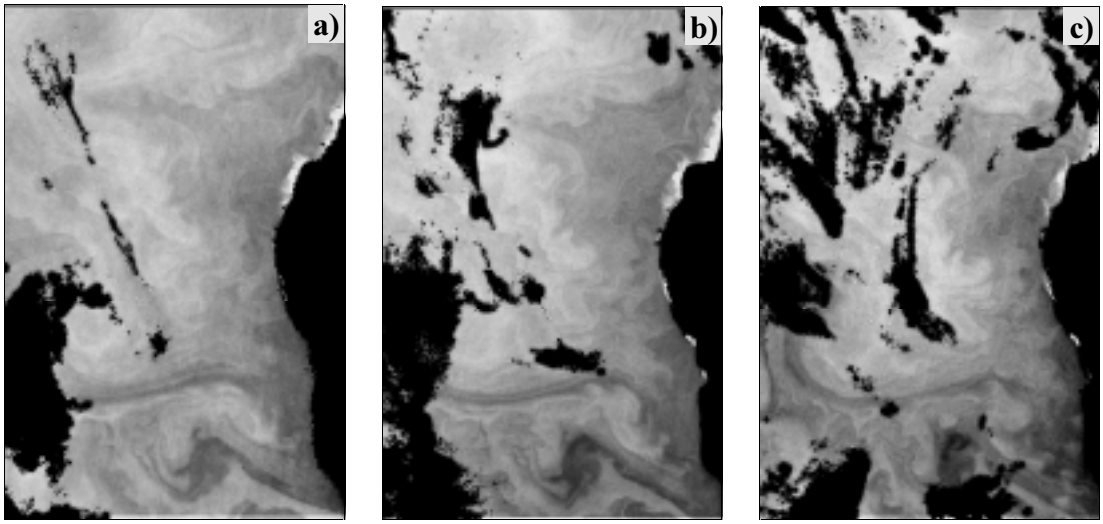

Images 9. Time serie of a the South-west coast of Madagascar : the 11th July (a), the 12th July (b), the 13th July (c), and the 16th July 2000 (d). The front very well pronounced on a, b, and c, is very consistent to the pigment concentration derived from SeaWiFS the 12th July (e). This front seems to correspond to high gradient of the sea level as seen on the weekly mean altimetry image of the 12th July (f).